

Probing maximal zero textures with broken cyclic symmetry in inverse seesaw

Rome Samanta*, Ambar Ghosal†

Saha Institute of Nuclear Physics, 1/AF Bidhannagar, Kolkata 700064, India

March 5, 2022

Abstract

Within the framework of inverse seesaw mechanism we investigate neutrino mass matrices invariant under cyclic symmetry (Z_3) with maximal zero texture (6 zero textures). We explore two different approaches to obtain the cyclic symmetry invariant form of the constituent matrices. In the first one we consider explicit cyclic symmetry in the neutrino sector of the Lagrangian which dictates the emerged effective neutrino mass matrix (m_ν) to be symmetry invariant and hence leads to a degeneracy in masses. We then consider explicit breaking of the symmetry through a dimensionless parameter ϵ' to remove the degeneracy. It is seen that the method doesn't support the current neutrino oscillation global fit data even after considering the correction from cyclic symmetry invariant charged lepton mass matrix (m_l) unless the breaking parameter is too large. In the second method, we assume the same forms of the neutrino mass matrices, however, symmetry is broken in the charged lepton sector. All the structures of the mass matrices are now dictated by an effective residual symmetry of some larger symmetry group in the Lagrangian. For illustration, we exemplify a toy model based on softly broken A_4 symmetry group which leads to one of the combination of m_l , m_D , M_{RS} and μ to generate effective m_ν . All the emerged mass matrices predict a constraint range of the CP violating phases and atmospheric mixing angle along with an inverted hierarchical structure of the neutrino masses. Further, significant

predictions on $\beta\beta 0\nu$ decay parameter $|m_{11}|$ and the sum of the three light neutrino masses ($\Sigma_i m_i$) are also obtained.

1 Introduction

Although Type-I seesaw has been most popularly used to generate light neutrino Majorana masses, the high scale introduced through the incorporation of heavy right chiral $SU(2)_L \times U(1)_Y$ singlet (ν_R) into this mechanism is beyond the reach of foreseeable collider experiments. Although the matter-antimatter asymmetry is naturally explained in this mechanism, lepton flavour violating process such as $\mu \rightarrow e\gamma$ are highly suppressed due to the new mass scale. An alternative to this scenario is to consider inverse seesaw mechanism [1–11] which contains additional left chiral $SU(2)_L \times U(1)_Y$ singlet field along with a low energy ($\sim \text{keV}$) lepton number violating mass matrix μ . The 9×9 neutrino mass matrix in this mechanism is written as

$$M_\nu = \begin{pmatrix} 0 & m_D & 0 \\ m_D^T & 0 & M_{RS} \\ 0 & M_{RS}^T & \mu \end{pmatrix} \quad (1)$$

with the choice of the basis (ν_L, ν_R^c, S_L) . After diagonalization the low energy effective neutrino mass matrix comes out as

$$\begin{aligned} m_\nu &= m_D M_{RS}^{-1} \mu (m_D M_{RS}^{-1})^T \\ &= F_\mu F^T \end{aligned} \quad (2)$$

*rome.samanta@saha.ac.in

†ambar.ghosal@saha.ac.in

where $F = m_D M_{RS}^{-1}$. Here m_D and M_{RS} are Dirac type whereas μ is Majorana type mass matrix. The key feature in inverse seesaw is that the matrix F plays an analogous role to that of m_D in conventional Type-I seesaw. Now if one choose $m_D \sim 100$ GeV and $M_{RS} \sim 10$ TeV, the light neutrino masses will be $\simeq 0.1$ eV which is protected by cosmology. Now due to the fewer number of experimental constraints a plausible approach is to minimize the number of parameters in the Lagrangian, in other words to consider maximal texture zeros [12–33] in the fundamental mass matrices. Furthermore, since all the low energy neutrino parameters have yet not been fixed, a large number of studies are devoted on imposing flavour symmetry in the Lagrangian to minimize the number of parameters. In the present work we adopt two different methods to incorporate the above ideas in the context of inverse seesaw mechanism. In the first method, to obtain viable neutrino mass matrix, we consider maximal zero textures along with a cyclic symmetry (Z_3)¹ between the generations of the neutrino fields motivated by the idea of Harrison, Perkins and Scott [34]. However, since cyclic symmetry gives rise to degenerate eigenvalues [35–37] it is necessary to lift the degeneracy and in the first method it is achieved through the minimal breaking of cyclic symmetry in M_{RS} matrix. However, in this scheme the charged lepton correction is unable to satiate all the oscillation data simultaneously. Motivated by the first one (as the neutrino mass matrices are highly constrained with minimum number of parameters), in the second method, we concentrate on cyclic symmetry invariant form of the neutrino mass matrices rather inquire to the explicit symmetry on the fields. Such type of form invariance can be realized through the residual symmetry [38–40] of some bigger symmetry group in the Lagrangian. To realize one of the sub case, as a toy model we exemplify a softly broken A_4 group as the bigger symmetry group which is completely broken in the charged lepton sector, though in the neutrino sector it breaks into Z_3 at the leading order. We particularly focus the cyclic symmetry (Z_3) invariant form of m_D and μ assuming diagonal M_{RS} in which residual Z_3 is broken. One of the combinations of the constituent matrices leads to a bi-maximal type mixing [41–46], therefore, to generate nonzero θ_{13} we appeal to the charged

lepton mass matrix which is not Z_3 invariant as well as in general non diagonal [47–50]. It is seen that the other emerged effective m_ν s also fail to explain the oscillation data unless charged lepton correction is considered.

The plan of the present work is as follows: Section 2 contains a qualitative description of the cyclic symmetry and texture zeros for two different methods considered. A numerical estimation to obtain the viable parameter space satisfying the oscillation data is presented in Section 3. Section 4 contains summary of the present work.

2 Cyclic symmetry and texture zeros

2.1 Explicit cyclic symmetry and texture zeros

We assume the following cyclic symmetry in ν_{iL} , ν_{iR} and S_{iL} fields as

$$\nu_{eL,R} \rightarrow \nu_{\mu L,R} \rightarrow \nu_{\tau L,R} \rightarrow \nu_{eL,R}, \quad (3)$$

$$S_{eL} \rightarrow S_{\mu L} \rightarrow S_{\tau L} \rightarrow S_{eL}. \quad (4)$$

After imposition of the above cyclic symmetry general Dirac and Majorana type mass matrices look like

$$m_D = \begin{pmatrix} y_1 & y_2 & y_3 \\ y_3 & y_1 & y_2 \\ y_2 & y_3 & y_1 \end{pmatrix}, M = \begin{pmatrix} x_1 & x_2 & x_2 \\ x_2 & x_1 & x_2 \\ x_2 & x_2 & x_1 \end{pmatrix}. \quad (5)$$

Now if we consider texture zeros along with the cyclic symmetry, clearly maximum number of zeros that can be accommodated within the above matrices are 6. In Table 1 all the 6 zero textures of m_D and M_{RS} are presented.

Since the low energy lepton number violating mass matrix μ is Majorana type therefore, only one texture with 6 zeros is possible and is given as

$$\mu^1 = \text{diag}(\mu_1, \mu_1, \mu_1). \quad (6)$$

Now, utilizing Eqn.(2) we construct m_ν and interestingly it is seen that along with diagonal μ any matrix presented in Table 1 can not generate phenomenologically viable m_ν , to be precise, all the emerged mass matrices (m_ν)

¹Motivation of considering cyclic symmetry is that at the leading order one of the diagonalizing matrix is U_{TBM} .

Table 1: Texture zeros with cyclic symmetry of m_D and M_{RS}

6 zero textures of m_D and M_{RS}					
$m_D^1 = \begin{pmatrix} y_1 & 0 & 0 \\ 0 & y_1 & 0 \\ 0 & 0 & y_1 \end{pmatrix}$		$M_{RS}^1 = \begin{pmatrix} M_1 & 0 & 0 \\ 0 & M_1 & 0 \\ 0 & 0 & M_1 \end{pmatrix}$			
$m_D^2 = \begin{pmatrix} 0 & y_2 & 0 \\ 0 & 0 & y_2 \\ y_2 & 0 & 0 \end{pmatrix}$		$M_{RS}^2 = \begin{pmatrix} 0 & M_2 & 0 \\ 0 & 0 & M_2 \\ M_2 & 0 & 0 \end{pmatrix}$			
$m_D^3 = \begin{pmatrix} 0 & 0 & y_3 \\ y_3 & 0 & 0 \\ 0 & y_3 & 0 \end{pmatrix}$		$M_{RS}^3 = \begin{pmatrix} 0 & 0 & M_3 \\ M_3 & 0 & 0 \\ 0 & M_3 & 0 \end{pmatrix}$			

are diagonal. We now consider the next maximal texture zero (3 zero) structure of μ , and is given by

$$\mu^2 = \begin{pmatrix} 0 & \mu_2 & \mu_2 \\ \mu_2 & 0 & \mu_2 \\ \mu_2 & \mu_2 & 0 \end{pmatrix}. \quad (7)$$

The above choice of μ matrix, along with the matrices presented in Table (1) enforces the m_ν to be nondiagonal. However, since the emerged m_ν is also cyclic symmetry invariant and hence leading to a degeneracy in the eigenvalues, therefore removal of the degeneracy requires a small breaking of the symmetry. Since our philosophy is to find out a viable texture with least number of parameters, we consider minimal symmetry breaking in the different elements of M_{RS} matrix only. For a compact view we present Table 2 which contains all the combinations and the corresponding neutrino mass matrices (m_ν) with

Table 2: Different Composition of m_D and μ matrices to generate m_ν .

m_D and μ		$M_{RS}^{1\epsilon}$	$M_{RS}^{2\epsilon}$	$M_{RS}^{3\epsilon}$
\Downarrow		m_ν		
m_D^1	μ^2	N^1	N^3	N^2
m_D^2	μ^2	N^2	N^1	N^3
m_D^3	μ^2	N^3	N^2	N^1
$m_D^{1,2,3}$	μ^1	$d^{1,2,3}$	$d^{3,1,2}$	$d^{2,3,1}$

the definitions $M_{RS}^{1\epsilon} = \text{diag}(M_1 + \epsilon, M_1, M_1)$, $M_{RS}^{2\epsilon} =$

$\text{diag}(M_1, M_1 + \epsilon, M_1)$, $M_{RS}^{3\epsilon} = \text{diag}(M_1, M_1, M_1 + \epsilon)$. The $d^{i(i=1,2,3)}_s$ are some diagonal matrices of not our concern as those are obtained due to 6 zero texture of μ as discussed earlier. The matrices N^1 , N^2 and N^3 arise due to 3 zero texture of μ matrix and explicitly their forms are given by

$$N^1 = \begin{pmatrix} 0 & A_1 & A_1 \\ A_1 & 0 & B_1 \\ A_1 & B_1 & 0 \end{pmatrix}, N^2 = \begin{pmatrix} 0 & B_2 & A_2 \\ B_2 & 0 & A_2 \\ A_2 & A_2 & 0 \end{pmatrix}, \quad (8)$$

$$N^3 = \begin{pmatrix} 0 & A_3 & B_3 \\ A_3 & 0 & A_3 \\ B_3 & A_3 & 0 \end{pmatrix}$$

with the definition of the parameters as

$$A_i = \frac{\mu_2 y_i^2}{M_1(M_1 + \epsilon)}, B_i = \frac{\mu_2 y_i^2}{M_1^2}. \quad (9)$$

Phenomenological consequences : As the left chiral neutrino fields obey cyclic symmetry, their charged lepton partners also follow the same. Hence, the charged lepton mass matrix (m_l) is diagonalized by trimaximal mixing matrix [38]. In the basis where the m_l is diagonal the effective neutrino mass matrix will be modified by the trimaximal mixing matrix. However, it is found that due to the lack of sufficient number of parameters, all the mixing angles cannot be obtained simultaneously in their 3σ range. We also consider the nondiagonal forms of M_{RS} matrices (i.e., all the possible cases given in Table 1) and find that the above conclusion is valid for all the cases. Now at this stage one could move one step ahead, i.e. one may consider three zero texture of m_D and M_{RS} . In that case all the constraints from the oscillation data can be accommodated undoubtedly. However, in such a scenario as the effective number of parameters in the m_ν itself (without considering the charged lepton correction) increase, thus, the predictions on the light neutrino masses (m_i), their sum ($\Sigma_i m_i$) and neutrinoless double beta decay parameter ($|m_{11}|$) are less significant (vary in a wide range). Thus, since the maximality of zeros is our concern, in the next section we present an alternative approach to preserve the maximal zero textures of the constituent neutrino mass matrices. In this approach the required texture zero mass matrices with cyclic symmetry in the neutrino sector and simple four zero textures with naturally broken Z_3 in the charged lepton sector are

realized from an effective residual symmetry to reproduce the forms of m_ν matrices presented in Table 2 .

2.2 Cyclic symmetry and texture zeros as an effective residual symmetry

In this section we present a toy model based on A_4 symmetry as a bigger symmetry group. Due to spontaneous breaking of A_4 , cyclic symmetry (Z_3) is preserved only in the neutrino sector while the charged lepton mass matrix is obtained with four zero Yukawa texture with decoupled third generation. Thus charged lepton correction also plays a crucial role to fit the extant data. However, before going into the detailed discussion, we would like to mention that although there are several cases in the analysis, we present a toy model only for one case. Furthermore, the symmetry group A_4 is not the only group to realize the cyclic symmetry with the texture zeros. Other symmetry groups such as S_4 , $U(1)_{B-L}$ etc. [38,51–53] can also lead to Z_3 invariance in the neutrino sector due to their spontaneous breaking. Now let us recall the problem we faced in the previous section. First, the maximal zero textures with cyclic symmetry in the neutrino sector do not entertain cyclic symmetry invariant form of the charged lepton mass matrix as far as the present experimental data is concerned. Apart from that one also needs to break cyclic symmetry in the neutrino sector since at the leading order it leads to a degeneracy in masses. Here, in the charged lepton sector, breaking of Z_3 is obtained due to spontaneous breaking of A_4 whereas in the neutrino sector the breaking scheme is similar to the previous section, i.e. the degeneracy is removed by due to a soft breaking term (ϵ) in the elements of M_{RS} . Thus we need the structure of M_{RS} due to minimal breaking as

$$M_{RS} = \text{diag} (M_1, M_2, M_2) \quad (10)$$

with $M_1 = M_2 + \epsilon$, to generate $N^{1,2,3}$ type mas matrices shown in Table 2. Obviously such choice of M_{RS} matrices with all nondegenerate eigenvalues are also consistent with the oscillation data. Although there are several effective m_ν arises due to suitable combinations of m_D , μ and M_{RS} , of them N^1 type matrix is a two parameter $\mu\tau$ symmetric matrix with zero diagonal entries. Consequently, the matrix leads to vanishing θ_{13} which is discarded by

the present oscillation data at $> 10\sigma$ level [54]. Thus to generate nonzero θ_{13} corrections from the charged lepton sector [47–50, 55] should be taken into account. As a simplistic scenario, in this section we consider corrections from all the three sectors of m_l . These simple structures of m_l are well motivated by popular discrete flavor groups which are used to explain neutrino mass and mixing. Here we consider A_4 as the flavor symmetry group. However, there are other groups, e.g. S_4 [56], Z_6 [50] etc. which can also lead to these structures of m_l . Interestingly, all the emerged m_ν which arises from $M_{RS} = \text{diag} (M_1, M_2, M_3)$ also require charged lepton correction which we discuss in the next section. Although there are several papers on A_4 symmetry we are motivated by Ref [11]. We discuss the required A_4 model in brief.

Table 3: Field content of the model with lepton and scalar assignment

	L	l_{lR}	N_{lR}	S_{lL}	ξ_{ch}, ϕ_{ch}	ξ_D	ξ_{RS}	ϕ_μ
$SU(2)_L$	2	1	1	1	2	2	1	1
Z_3	ω	1	ω	ω^2	ω	1	ω	ω^2
Z_2	+	+	–	+	+	–	–	+
A_4	3	3	3	3	1, 3	1	1	3

Fermionic part of the Lagrangian consists of four part as shown below

$$\mathcal{L}_{mass}^{A_4} = \mathcal{L}_{ch} + \mathcal{L}_{Dirac} + \mathcal{L}_{RS} + \mathcal{L}_{ss}. \quad (11)$$

Explicitly each term is written as

$$\begin{aligned} \mathcal{L}_{mass}^{A_4} = & Y_{ch} \bar{L} l_R (\phi_{ch} + \xi_{ch}) + Y_D \bar{L} N_R \xi_D \\ & + Y_M \bar{S}_L N_R \xi_{RS} + Y_u \bar{S}_L^C S_L \phi_\mu + \text{h.c} \end{aligned} \quad (12)$$

with the following choice of the alignment $\xi_{ch} \sim < v_{ch}^\xi >$, $\phi_{ch} \sim < 0, 0, v_{ch}^\phi >$, $\xi_D \sim < v_D^\xi >$, $\xi_{RS} \sim < v_{RS}^\xi >$ and $\phi_\mu \sim < v_\mu^\phi, v_\mu^\phi, v_\mu^\phi >$. With such choice of VEV one can realize the charged lepton correction from 1 – 2 sector and the structures of m_D^1 and μ^2 along with the structure of M_{RS} as

$$M_{RS} = \text{diag}(M, M, M). \quad (13)$$

Here we assume A_4 group is generated by two generators

$$S = \begin{pmatrix} 1 & 0 & 0 \\ 0 & -1 & 0 \\ 0 & 0 & -1 \end{pmatrix}, \quad T = \begin{pmatrix} 0 & 1 & 0 \\ 0 & 0 & 1 \\ 1 & 0 & 0 \end{pmatrix}. \quad (14)$$

The three dimensional representation satisfy the product rule

$$3 \times 3 = 1 + 1' + 1'' + 3_S + 3_A \quad (15)$$

where

$$1 = a_1 b_1 + a_2 b_2 + a_3 b_3 \quad (16)$$

$$1' = a_1 b_1 + \omega^2 a_2 b_2 + \omega a_3 b_3 \quad (17)$$

$$1'' = a_1 b_1 + \omega a_2 b_2 + \omega^2 a_3 b_3 \quad (18)$$

and

$$3_S = \left(\frac{a_2 b_3 + a_3 b_2}{2}, \frac{a_3 b_1 + a_1 b_3}{2}, \frac{a_1 b_2 + a_2 b_1}{2} \right) \quad (19)$$

$$3_A = \left(\frac{a_2 b_3 - a_3 b_2}{2}, \frac{a_3 b_1 - a_1 b_3}{2}, \frac{a_1 b_2 - a_2 b_1}{2} \right). \quad (20)$$

Thus, A_4 is spontaneously broken in the charged lepton sector such that there is no effective Z_3 symmetry, however, the neutrino sector enjoys an effective residual Z_3 symmetry. As previously mentioned, Z_3 in M_{RS} should be broken, we consider soft A_4 breaking term in the Lagrangian which is well studied earlier [57–59]. We consider \mathcal{L}^{soft} as

$$\mathcal{L}^{soft} = \epsilon_{\alpha\beta} \bar{S}_{\alpha L} N_{\beta R} \quad (21)$$

where $\epsilon_{\alpha\beta}$ ($\alpha, \beta=1,2,3$) is a coupling constant with mass dimension one and the double indices do not mean the summation over the indices. The term contributes to the (α, β) element of M_{RS} and breaks the residual Z_3 symmetry. Now if we choose $(\alpha, \beta = 1)$ then the soft term contributes to (1,1) element of M_{RS} which in turn generates N^1 type m_ν with m_D^1 and μ^2 . In the following two sections we present detailed analysis of all the emerged m_ν .

2.2.1 Two degenerate eigenvalues of M_{RS}

The matrix of type $N^{1,2,3}$ can be realized by changing the nondegenerate value at three different diagonal entries

of M_{RS} matrix given in Eqn.(10 along with m_D^1 and μ^2 . First we consider the N^1 matrix which is given by

$$N^1 = m_\nu = \begin{pmatrix} 0 & yp & yp \\ yp & 0 & y \\ yp & y & 0 \end{pmatrix} \quad (22)$$

with $y = \mu_2 y_1^2 / M_2^2$, $p = M_2 / M_1$. The matrix of Eqn. (22) is diagonalized by the unitary mixing matrix U_ν given by

$$U_\nu = \begin{pmatrix} c_{12} & s_{12} & 0 \\ -\frac{1}{\sqrt{2}} s_{12} & \frac{1}{\sqrt{2}} c_{12} & -\frac{1}{\sqrt{2}} \\ -\frac{1}{\sqrt{2}} s_{12} & \frac{1}{\sqrt{2}} c_{12} & \frac{1}{\sqrt{2}} \end{pmatrix} \quad (23)$$

where

$$c_{12} = \frac{\sqrt{1 + \frac{1}{\sqrt{1+8p^2}}}}{\sqrt{2}}$$

and

$$s_{12} = \sqrt{\frac{1}{2} - \frac{1}{2\sqrt{1+8p^2}}}. \quad (24)$$

Interestingly, if $p \rightarrow \infty$ ($M_2 \gg M_1$) we can have the well known bi-maximal mixing of neutrino masses. The eigenvalues of m_ν are given by

$$\begin{aligned} -m_1 &= \frac{1}{2}(y - \sqrt{1+8p^2}y) \\ m_2 &= \frac{1}{2}(y + \sqrt{1+8p^2}y) \\ -m_3 &= -y \end{aligned} \quad (25)$$

where $m_2 > m_1 > m_3$. Now defining $\Delta m_{sol}^2 = m_2^2 - m_1^2$ and $\Delta m_{atm}^2 = m_2^2 - m_3^2$ we get an explicit relationship between Δm_{sol}^2 and Δm_{atm}^2 as

$$\Delta m_{atm}^2 = \frac{1}{2} \frac{\Delta m_{sol}^2}{\sqrt{1+8p^2}} (4p^2 - 1) + \frac{\Delta m_{sol}^2}{2} \quad (26)$$

from which we obtain an approximate range for p through the experimental inputs of 3σ ranges. In order to generate nonzero θ_{13} we invoke contribution from the charged lepton sector in the following way. We consider Altarelli-Ferugilo-Masina

parametrization [60] for U_{PMNS} which is written as $U_{PMNS} = U_l^\dagger U_\nu = \tilde{U}_l^\dagger \text{diag}(-e^{i\phi_1}, e^{i\phi_2}, 1) U_\nu \times \text{diag}(1, e^{i\alpha}, e^{i(\beta+\delta_{CP})})$, where U_l diagonalizes the charged lepton mass matrix and \tilde{U}_l follows usual CKM type parametrization as

$$\tilde{U}_l = \tilde{R}(\theta_{23}) \tilde{R}(\theta_{13}, \delta) \tilde{R}(\theta_{12}) \quad (27)$$

with

$$\begin{aligned} \tilde{R}(\theta_{23}) &= \begin{pmatrix} 1 & 0 & 0 \\ 0 & \sqrt{1-\lambda_{23}^2} & \lambda_{23} \\ 0 & -\lambda_{23} & \sqrt{1-\lambda_{23}^2} \end{pmatrix}, \\ \tilde{R}(\theta_{13}, \delta) &= \begin{pmatrix} \sqrt{1-\lambda_{13}^2} & 0 & \lambda_{13}e^{i\delta} \\ 0 & 1 & 0 \\ -\lambda_{13}e^{-i\delta} & 0 & \sqrt{1-\lambda_{13}^2} \end{pmatrix} \\ \text{and } \tilde{R}(\theta_{12}) &= \begin{pmatrix} \sqrt{1-\lambda_{12}^2} & \lambda_{12} & 0 \\ -\lambda_{12} & \sqrt{1-\lambda_{12}^2} & 0 \\ 0 & 0 & 1 \end{pmatrix} \end{aligned} \quad (28)$$

along with $\lambda_{ij} = \sin \theta_{ij}$.

As we are considering CKM type mixing matrix therefore, we expect small mixing in the charged lepton sector. Moreover the small value of reactor mixing angle also enforces the value of λ to be small. The textures of the charged lepton mass matrices are presented in Table 4 where ‘ \times ’ corresponds to some nonzero entries in m_l . Considering $|e_{\alpha=(e,\mu,\tau)}\rangle$ to be the flavour eigenstate and $|e_i\rangle$ the mass eigenstate of the charged leptons we address three possible cases corresponding to the three textures of m_l for modifications of U_ν .

Case I: $|e_\tau\rangle^{flavour} = |e_i\rangle^{mass}, m_l \Rightarrow m_l^{12}$

In this case U_ν is modified by the 1-2 sector ($\tilde{R}(\theta_{12})$) of

U_l and the elements of U_{PMNS} can be written as

$$\begin{aligned} U_{11} &= -e^{i\phi_1} \sqrt{1-\lambda_{12}^2} c_{12} - \frac{1}{\sqrt{2}} \lambda_{12} e^{i\phi_2} s_{12} \\ U_{12} &= -e^{i\phi_1} \sqrt{1-\lambda_{12}^2} s_{12} + \frac{1}{\sqrt{2}} \lambda_{12} e^{i\phi_2} c_{12}, \\ U_{13} &= -\frac{1}{\sqrt{2}} \lambda_{12} e^{i\phi_2} \\ U_{22} &= -\lambda_{12} e^{i\phi_1} s_{12} + \frac{1}{\sqrt{2}} \sqrt{1-\lambda_{12}^2} e^{i\phi_2} c_{12} \\ U_{23} &= -\frac{1}{\sqrt{2}} \sqrt{1-\lambda_{12}^2} e^{i\phi_2}, U_{33} = \frac{1}{\sqrt{2}} \end{aligned} \quad (29)$$

and hence the three mixing angles come out as

$$\begin{aligned} \sin \theta_{13} &= |U_{13}| = \frac{\lambda_{12}}{\sqrt{2}} \\ \tan \theta_{12} &= \frac{|U_{12}|}{|U_{11}|} = \frac{s_{12}(s_{12} - \sqrt{2} \cos[\phi_1 - \phi_2] c_{12} \lambda_{12})}{c_{12}(c_{12} + \sqrt{2} \cos[\phi_1 - \phi_2] s_{12} \lambda_{12})} \\ \tan \theta_{23} &= \frac{|U_{23}|}{|U_{33}|} = \sqrt{1-\lambda_{12}^2}. \end{aligned} \quad (30)$$

The measure of CP violation J_{CP} can be written in terms of the mixing matrix elements as

$$J_{CP} = \frac{\sin(\phi_2 - \phi_1) c_{12} s_{12} \lambda_{12}}{2\sqrt{2}} \quad (31)$$

and hence the Dirac CP phase δ_{CP} is obtained as

$$\sin \delta_{CP} = \frac{J_{CP}}{\Omega} \quad (32)$$

with the definition of Ω as

$$\Omega = c'_{12} c'^2_{13} c'_{23} s'_{12} s'_{13} s'_{23} \quad (33)$$

where $s'_{ij} \Rightarrow \sin \theta_{ij}$ and $c'_{ij} \Rightarrow \cos \theta_{ij}$ are the usual mixing parameters in the CKM part of U_{PMNS} which is defined as

$$U_{PMNS} = P_\alpha U_{CKM} P_M \quad (34)$$

with $P_\alpha = \text{diag}(e^{i\alpha_1}, e^{i\alpha_2}, e^{i\alpha_3})$ as the unphysical phase matrix, $U_{CKM} = \tilde{U}_l^\dagger \text{diag}(-e^{i\phi_1}, e^{i\phi_2}, 1) U_\nu$ and $P_M = \text{diag}(1, e^{i\alpha}, e^{i(\beta+\delta_{CP})})$ as the Majorana phase matrix.

Table 4: Textures of the charged lepton mass matrix (m_l)

4 zero textures of m_l		
$m_l^{12} = \begin{pmatrix} \times & \times & 0 \\ \times & \times & 0 \\ 0 & 0 & \times \end{pmatrix}$	$m_l^{13} = \begin{pmatrix} \times & 0 & \times \\ 0 & \times & 0 \\ \times & 0 & \times \end{pmatrix}$	$m_l^{23} = \begin{pmatrix} \times & 0 & 0 \\ 0 & \times & \times \\ 0 & \times & \times \end{pmatrix}$

We use other two rephasing invariant quantities to calculate the Majorana phases as [47]

$$\begin{aligned}\alpha &= \arg(U_{11}^* U_{12}) \\ \beta &= \arg(U_{13} U_{11}^*)\end{aligned}\quad (35)$$

and thereby the phases come out as

$$\tan \alpha = \frac{\sqrt{2} \sin(\phi_2 - \phi_1) \lambda_{12}}{\sqrt{2} \cos(\phi_2 - \phi_1) (c_{12}^2 - s_{12}^2) \lambda_{12} - 2c_{12}s_{12}} \quad (36)$$

and

$$\tan \beta = \frac{\sin(\phi_2 - \phi_1) c_{12}}{\sqrt{2} \cos(\phi_2 - \phi_1) c_{12} + s_{12} \lambda_{12}}. \quad (37)$$

Case II: $|e_\mu\rangle^{flavour} = |e_i\rangle^{mass}$, $m_l \Rightarrow m_l^{13}$

In this case modification to U_ν originates from 1-3 sector ($\tilde{R}(\theta_{13}, \delta)$) of U_l and the elements of U_{PMNS} can be written as

$$\begin{aligned}U_{11} &= -e^{i\phi_1} \sqrt{1 - \lambda_{13}^2} c_{12} - \frac{1}{\sqrt{2}} \lambda_{13} e^{i\delta} s_{12} \\ U_{12} &= -e^{i\phi_1} \sqrt{1 - \lambda_{13}^2} s_{12} + \frac{1}{\sqrt{2}} \lambda_{13} e^{i\delta} c_{12}, \\ U_{13} &= -\frac{1}{\sqrt{2}} \lambda_{13} e^{i\delta} \\ U_{22} &= \frac{1}{\sqrt{2}} c_{12}, U_{23} = -\frac{1}{\sqrt{2}}, U_{33} = \frac{1}{\sqrt{2}} \sqrt{1 - \lambda_{13}^2}\end{aligned} \quad (38)$$

and hence the three mixing angles come out as

$$\begin{aligned}\sin \theta_{13} &= |U_{13}| = \frac{\lambda_{13}}{\sqrt{2}} \\ \tan \theta_{12} &= \frac{|U_{12}|}{|U_{11}|} = \frac{s_{12}(s_{12} - \sqrt{2} \cos[\delta - \phi_1] c_{12} \lambda_{13})}{c_{12}(c_{12} + \sqrt{2} \cos[\delta - \phi_1] s_{12} \lambda_{13})} \\ \tan \theta_{23} &= \frac{|U_{23}|}{|U_{33}|} = \frac{1}{\sqrt{1 - \lambda_{13}^2}}.\end{aligned} \quad (39)$$

Proceeding in the same way as discussed in **Case I**, J_{CP} can be written in terms of the mass matrix elements as

$$J_{CP} = \frac{\sin(\phi_1 - \delta) c_{12} s_{12} \lambda_{13}}{2\sqrt{2}} \quad (40)$$

and

$$\sin \delta_{CP} = \frac{J_{CP}}{\Omega} \quad (41)$$

where Ω is already defined in Eqn (33). Finally the Majorana phases are calculated as

$$\tan \alpha = \frac{\sqrt{2} \sin(\delta - \phi_1) \lambda_{13}}{\sqrt{2} \cos(\delta - \phi_1) (c_{12}^2 - s_{12}^2) \lambda_{13} - 2c_{12}s_{12}} \quad (42)$$

and

$$\tan \beta = \frac{\sin(\delta - \phi_1) c_{12}}{\sqrt{2} \cos(\delta - \phi_1) c_{12} + s_{12} \lambda_{13}}. \quad (43)$$

Case III: $|e_e\rangle^{flavour} = |e_i\rangle^{mass}$, $m_l \Rightarrow m_l^{23}$

For this texture of m_l (alternatively $\tilde{R}(\theta_{23})$ as the mixing matrix) it is not possible to generate θ_{13} , hence is not taken into account.

We also consider the other two matrices N^2 and N^3 and obtained all the mixing angles and eigenvalues. However, from numerical estimation it is found that both the cases do not admit the present experimental data and hence discarded.

2.2.2 All nondegenerate eigenvalues of M_{RS}

Taking three different 6 zero textures of $m_D(m_D^{1,2,3})$ and one 3 zero texture of $\mu(\mu^2)$ with the M_{RS} as

$$M_{RS} = \text{diag}(M_1, M_2, M_3) \quad (44)$$

we construct three different textures of m_ν using inverse seesaw formula and they lead to

$$m_\nu^1 = \begin{pmatrix} 0 & yp & ypq \\ yp & 0 & yq \\ ypq & yq & 0 \end{pmatrix}, m_\nu^2 = \begin{pmatrix} 0 & yq & yp \\ yq & 0 & ypq \\ yp & ypq & 0 \end{pmatrix},$$

$$m_\nu^3 = \begin{pmatrix} 0 & ypq & yq \\ ypq & 0 & yq \\ yq & yp & 0 \end{pmatrix} \quad (45)$$

where $p = M_2/M_1$ and $q = M_2/M_3$ and $y = \mu y_i^2/M_2^2$ for each m_ν^i . Now in the basis where the charged lepton mass matrix is diagonal one can easily construct the effective m_ν s as

$$m_{\nu f} = U_l^\dagger m_\nu^i U_l^* \quad (46)$$

where U_l is already defined in Section 2.2.1. Since we are considering three specific textures of the charged lepton mass matrices (Table 4), therefore, for a given m_ν we can construct three $m_{\nu f}$ taking contribution from each sectors of the charged leptons. Hence, we have altogether 9 effective $m_{\nu f}$. We consistently denote them as $m_{\nu f ij}$ after getting correction from the ' ij 'th sector of U_l . We do not present explicit structures of all the mass matrices. However, numerical estimation for each viable matrix is presented in the next section.

3 Numerical analysis and phenomenological discussion

i) Two degenerate eigenvalues of M_{RS}

Before going into the details of the numerical analysis an important point is to be noted that except $\tan \theta_{23}$ the expressions for the physical parameters obtained in Case II are the same as that of the Case I if we replace λ_{13} by λ_{12} and δ by ϕ_2 and therefore the numerical estimation for one case can be automatically translated to the other. Therefore from now on in a generic way we rename λ_{12} and λ_{13} as λ .

We consider small mixing arises from the charged lepton sector and accordingly written down the expressions for the physical parameters with the terms dominant in λ . Moreover, the smallness of θ_{13} automatically implies that the order of λ should be of the order of Sine of the reactor

Table 5: Input experimental values [61]

Quantity	3σ ranges
$ \Delta m_{31}^2 $ (N)	$2.30 < \Delta m_{31}^2 (10^3 eV^{-2}) < 2.64$
$ \Delta m_{31}^2 $ (I)	$2.20 < \Delta m_{31}^2 (10^3 eV^{-2}) < 2.54$
Δm_{21}^2	$7.11 < \Delta m_{21}^2 (10^5 eV^{-2}) < 8.18$
θ_{12}	$31.8^\circ < \theta_{12} < 37.8^\circ$
θ_{23}	$39.4^\circ < \theta_{23} < 53.1^\circ$
θ_{13}	$8^\circ < \theta_{13} < 9.4^\circ$

mixing angle. Taking into account the neutrino oscillation global fit data presented in Table 5 we randomly vary λ and $\phi_2 - \phi_1$ within the ranges as $0 < \lambda < 0.3$ and $-180^\circ < \phi_2 - \phi_1 < 180^\circ$ and scan the parameter space. It is seen that the matrices of type N^2 and N^3 are not phenomenologically viable (even after considering charged lepton contribution) as far as the present neutrino oscillation data is concerned. For N^1 type matrix we plot in figure 1 the variation of p Vs y , λ Vs $\phi_2 - \phi_1$ and λ Vs θ_{13} and it is depicted from the plots that the parameters y and p vary within the ranges as $0.00071 < y < 0.00087$ and $38 < p < 51$ which is presented in the extreme left of figure 1. The ranges of λ and $\phi_2 - \phi_1$ are obtained as $0.197 < \lambda < 0.231$ and $35.5^\circ < \phi_2 - \phi_1 < 74^\circ$, $-35.5^\circ < \phi_2 - \phi_1 < -74^\circ$ as one can read from the middle plot of figure 1. Now since $|U_{e3}|$ is directly proportional to λ it is needless to say that there is a linear variation of $|U_{e3}|$ with λ and is depicted in the last plot of figure 1. As $\tan \theta_{12}$ has a strong dependence on $\phi_2 - \phi_1$ we also present the variation of θ_{12} with $\phi_2 - \phi_1$ in the extreme right panel of figure 2. The atmospheric mixing angle θ_{23} doesn't deviate much from 45° . For Case I, θ_{23} is smaller than the bi-maximal value while for the Case II it is slightly enhanced and we plot them in the first two figures of figure 2. This is a distinguishable characteristic between the two cases. Now as the CP violation in U_{PMNS} is solely controlled by the phases arising from the charged lepton sector therefore we expect a great dependency of δ_{CP} on $\phi_2 - \phi_1$ ($\delta - \phi_1$ for Case II) and a correlation between the CP phases. We plot δ_{CP} with $\phi_2 - \phi_1$ in the extreme left panel of figure 3 while the correlation of the Majorana phases with δ_{CP} is shown in the other two figures of figure 3. The ranges of the Dirac

CP phase δ_{CP} is obtained as $38^\circ < |\delta_{CP}| < 85^\circ$ while the Majorana phases are constrained as $30^\circ < |\beta| < 65^\circ$ and $8^\circ < |\alpha| < 17^\circ$. The J_{CP} value is obtained within the range as $0.017 < |J_{CP}| < 0.04$ as one can read from the extreme left plot of figure 4. The model predicts inverted hierarchy of the neutrino masses which is explicit from the second figure of figure 4. We also obtain a range on the sum of three light neutrino masses as $0.0953 \text{ eV} < \Sigma_i m_i < 0.1026 \text{ eV}$ and a range of $|m_{11}|$ as $0.03 \text{ eV} < |m_{11}| < 0.048 \text{ eV}$ which are well below the present experimental upper bound 0.23 eV and 0.35 eV respectively [62].

Before closing the discussion we would like to mention that although charged lepton correction to $\mu\tau$ symmetric matrix is studied before [47–50], here we consider a two parameter structure of a $\mu\tau$ symmetric matrix which is much more predictive than the previous ones. As for example in our model CP violation arises completely from the charged lepton sector as our mass matrix consist of two real parameters. Thus mixing in the charged lepton sector dictates a common origin of θ_{13} and the CP-violating phases. In our analysis the Dirac and Majorana phases are significantly correlated. Thus only the measurement of CP violating phases can challenge the viability of the present model [56]. With the recent hint of T2K, nearly maximal CP violation [63] is also allowed here which in turn fixes the Majorana phases and thus the double beta decay parameter $|m_{11}|$. The allowed occurrence of inverted hierarchy puts a lower limit to $|m_{11}|$ as shown in figure 5. One can see a very narrow range of $|m_{11}|$ is allowed. Thus significant development of the experiments like GERDA and EXO can test the viability of the model. Finally the constraint range of the sum of the light neutrino masses is also a major result of the analysis as $\Sigma_i m_i \sim 0.1 \text{ eV}$ at 4σ level is expected to be probed by the future astrophysical experiments.

ii) All nondegenerate eigenvalues of M_{RS}

In this category there are 9 structures of effective m_ν matrices. We diagonalize them through a direct diagonalization procedure [35] and calculate the eigenvalues, mixing angles. It is seen that the matrices $m_{\nu f23}^1$, $m_{\nu f23}^2$ and $m_{\nu f23}^3$ are phenomenologically ruled out. To be more specific one needs $\lambda_{23} \gg 1$ which is not the case. Proceeding in the same way as that of the previous section we estimate the ranges of J_{CP} , δ_{CP} , α , β , $|m_{11}|$ and $|\Sigma_i m_i|$

for the survived matrices. The hierarchy of the neutrino masses for all the cases is inverted. The predictions of the viable matrices are listed in Table 6. In figure 6 we plot the lightest eigenvalue with $|m_{11}|$.

Before concluding this section we would like to mention that the charged lepton correction to the matrices given in Eqn. (45) (with all diagonal entries zero) are also studied in Ref. [16]. Particularly the classes 4_4 and 3_1 [16] respectively resemble m_l and m_ν matrices considered here in the present work. However, in Ref. [16] these cases are categorized as less predictive due to large number of parameters (10 real parameters) and hence the results are not presented. However in the present work, those cases contain less number of parameters (7 real parameters) since the structure of M_{RS} matrix is flavour diagonal (p and q parameters defined in Section 2.2.2 are real) and we estimate the prediction for these cases regarding $|m_{11}|$, $\Sigma_i m_i$, δ_{CP} etc.

Some concluding remarks regarding predictions of the present scheme:

1. We see the hierarchy of neutrino mass predicted in all the cases is inverted. This can be testified in the near future through the combined analysis of NO ν A and T2K [64] experimental data with the aid of the knowledge of precise θ_{13} . The Majorana phases do not appear in *neutrino* \rightarrow *neutrino* oscillation experiments, however, they may appear in *neutrino* \rightarrow *anti neutrino* oscillation experiments. Although these experiments are difficult to design, however, in an optimistic point of view we expect the prediction for the Majorana phases in this model will also be tested in future experiments.
2. The predicted value of $\Sigma_i m_i$ obtained in the present model could also be tested in the near future through more precise estimation of $\Sigma_i m_i$ due to a combined analysis using PLANCK data [62] and other cosmological and astrophysical experiments [65, 66]. The value of $\Sigma_i m_i \sim 0.1 \text{ eV}$ at the 4σ level could be probed through such analysis for the inverted ordering of the neutrino masses.
3. The Dirac CP phase δ_{CP} predicted in this work will be tested at NO ν A, T2K and DUNE [67] in near future.

4 Summary and Conclusion

Within the framework of inverse seesaw, we study the phenomenology of maximal zero textures and cyclic

symmetry in the neutrino matrices. We adopt two different schemes to accommodate the present oscillation data. In the first approach we consider explicit cyclic symmetry on the relevant fields which leads to degenerate eigenvalues. To remove the degeneracy in the eigenvalues we incorporate explicit symmetry breaking term in the Lagrangian. It is seen that even after considering the charged lepton correction from the cyclic symmetry invariant m_l , present oscillation data can not be explained and hence the first approach is discarded. In the second one, we concentrate on the same form of the neutrino mass matrices which can be realized through an effective residual symmetry of some bigger symmetry group in the Lagrangian, in which cyclic symmetry in the charged lepton sector is broken after spontaneous breaking of the bigger group. Further we exemplify a toy model with softly broken A_4 symmetry to realize one of the combinatorial structure of effective m_ν . To fit the oscillation data charged lepton correction from different sectors of U_l is considered along with a soft breaking term in M_{RS} which removes the degeneracy in masses. Each cases predict a highly constrained ranges of CP violating phases, $|m_{11}|$ and $\Sigma_i m_i$ along with inverted ordering of the neutrino masses.

Acknowledgement

Authors acknowledge Department of Atomic Energy (DAE), Government of India, for financial support.

References

- [1] R. N. Mohapatra and J. W. F. Valle, Phys. Rev. D **34**, 1642 (1986).
- [2] J. Bernabeu, A. Santamaria, J. Vidal, A. Mendez and J. W. F. Valle, Phys. Lett. B **187**, 303 (1987).
- [3] R. N. Mohapatra, Phys. Rev. Lett. **56**, 561 (1986).
- [4] J. Schechter and J. W. F. Valle, Phys. Rev. D **25**, 774 (1982).
- [5] J. Schechter and J. W. F. Valle, Phys. Rev. D **22**, 2227 (1980).
- [6] S. Fraser, E. Ma and O. Popov, Phys. Lett. B **737**, 280 (2014) [arXiv:1408.4785 [hep-ph]].
- [7] H. Hettmansperger, M. Lindner and W. Rodejohann, JHEP **1104**, 123 (2011) [arXiv:1102.3432 [hep-ph]].
- [8] B. Adhikary, A. Ghosal and P. Roy, Indian J. Phys. **88**, 979 (2014) [arXiv:1311.6746 [hep-ph]].
- [9] S. S. C. Law and K. L. McDonald, Phys. Rev. D **87**, no. 11, 113003 (2013) [arXiv:1303.4887 [hep-ph]].
- [10] P. S. B. Dev and R. N. Mohapatra, Phys. Rev. D **81**, 013001 (2010) [arXiv:0910.3924 [hep-ph]].
- [11] M. Hirsch, S. Morisi and J. W. F. Valle, Phys. Lett. B **679**, 454 (2009) [arXiv:0905.3056 [hep-ph]].
- [12] W. Grimus, A. S. Joshipura, L. Lavoura and M. Tanimoto, Eur. Phys. J. C **36**, 227 (2004) [hep-ph/0405016].
- [13] S. Dev, S. Gupta and R. R. Gautam, Phys. Lett. B **701**, 605 (2011) [arXiv:1106.3451 [hep-ph]].
- [14] P. H. Frampton, S. L. Glashow and D. Marfatia, Phys. Lett. B **536**, 79 (2002) [hep-ph/0201008].
- [15] K. Whisnant, J. Liao and D. Marfatia, AIP Conf. Proc. **1604**, 273 (2014).
- [16] P. O. Ludl and W. Grimus, JHEP **1407**, 090 (2014) [arXiv:1406.3546 [hep-ph]].
- [17] W. Grimus and P. O. Ludl, PoS EPS -HEP2013, 075 (2013) [arXiv:1309.7883 [hep-ph]].
- [18] J. Liao, D. Marfatia and K. Whisnant, JHEP **1409**, 013 (2014) [arXiv:1311.2639 [hep-ph]].
- [19] H. Fritzsch, Z. z. Xing and S. Zhou, JHEP **1109**, 083 (2011) [arXiv:1108.4534 [hep-ph]].
- [20] A. Merle and W. Rodejohann, Phys. Rev. D **73**, 073012 (2006) [hep-ph/0603111].
- [21] W. Wang, Eur. Phys. J. C **73**, 2551 (2013) [arXiv:1306.3556 [hep-ph]].
- [22] W. Wang, Phys. Lett. B **733**, 320 (2014) [Erratum-ibid. B **738**, 524 (2014)] [arXiv:1401.3949 [hep-ph]].
- [23] L. Lavoura, Phys. Lett. B **609**, 317 (2005) [hep-ph/0411232].

Table 6: Predictions of the viable matrices.

	Six predicted quantities					
	$ \delta_{CP} $ (deg.)	$ \alpha $ (deg.)	$ \beta $ (deg.)	$ J_{CP} $	$\Sigma_i m_i$ (eV)	$ m_{11} $ (eV)
$m_{\nu f12}^1$	100 – 23	–80 – 12	–63 – 23	0.01 – 0.04	0.09 – 0.12	0.026 – 0.048
$m_{\nu f12}^2$	98 – 34	92 – 18	78 – 0	0.015 – 0.38	0.07 – 0.108	0.029 – 0.049
$m_{\nu f12}^3$	88 – 0	71 – 37	62 – 35	0.012–0.036	0.07 – 0.1	0.029 – 0.048
$m_{\nu f13}^1$	100 – 20	85 – 10	60 – 20	0.01 – 0.04	0.09 – 0.14	0.031 – 0.05
$m_{\nu f13}^2$	94 – 35	100 – 18	81 – 14	0.012–0.038	0.07 – 0.132	0.032 – 0.049
$m_{\nu f13}^3$	102 – 17	82 – 26	62 – 21	0.017 – 0.04	0.08 – 0.15	0.028 – 0.048

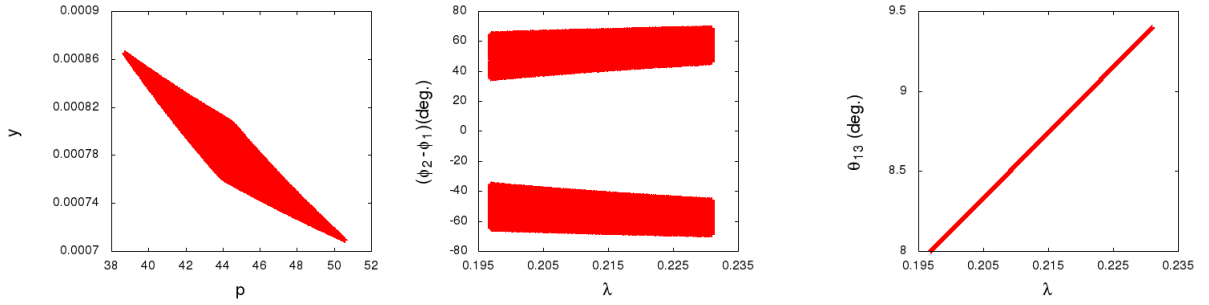


Figure 1: (colour online) Correlation plots: Extreme left plot represents y Vs p while the middle one shows λ Vs $\phi_2 - \phi_1$ for Case I. For Case II we get the same plot just by replacing $\phi_2 - \phi_1$ with $\delta - \phi_1$ and finally the plot in the extreme right shows the variation of λ with θ_{13} for both the cases.

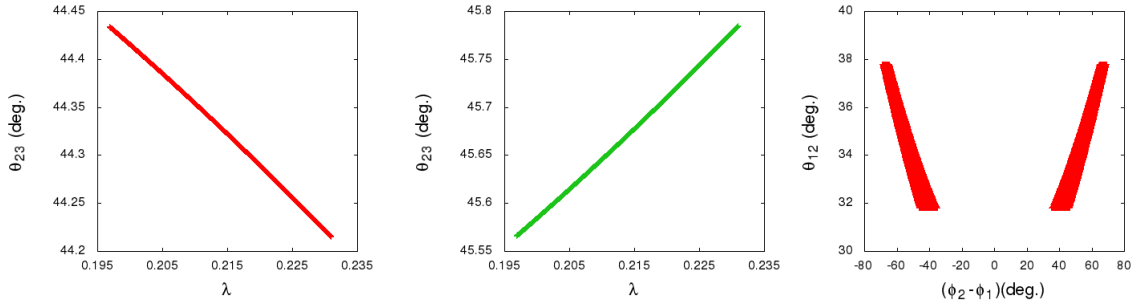


Figure 2: (colour online) The first figure (the red line) shows the variation of the atmospheric mixing angle (θ_{23}) with λ for Case I while the second one (the green line) shows the same for Case II. The last one represents the correlation between θ_{12} and $\phi_2 - \phi_1$ for case I. We get the same plot for case II by replacing $\phi_2 - \phi_1$ with $\delta - \phi_1$.

- [24] A. Kageyama, S. Kaneko, N. Shimoyama and M. Tanimoto, Phys. Lett. B **538**, 96 (2002) [hep-ph/0204291]. [25] W. Wang, Phys. Rev. D **90**, 033014 (2014) [arXiv:1402.6808 [hep-ph]].

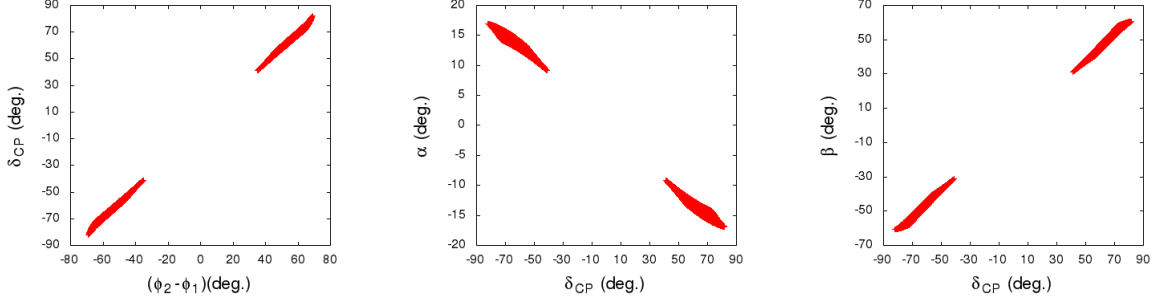


Figure 3: (colour online) The plot in the extreme left side shows the variation of $\phi_2 - \phi_1$ with δ_{CP} for Case I and we get the same plot for Case II by replacing $\phi_2 - \phi_1$ with $\delta - \phi_1$ while the other two plots show the correlation between the Majorana phases with δ_{CP} and are same for both the cases.

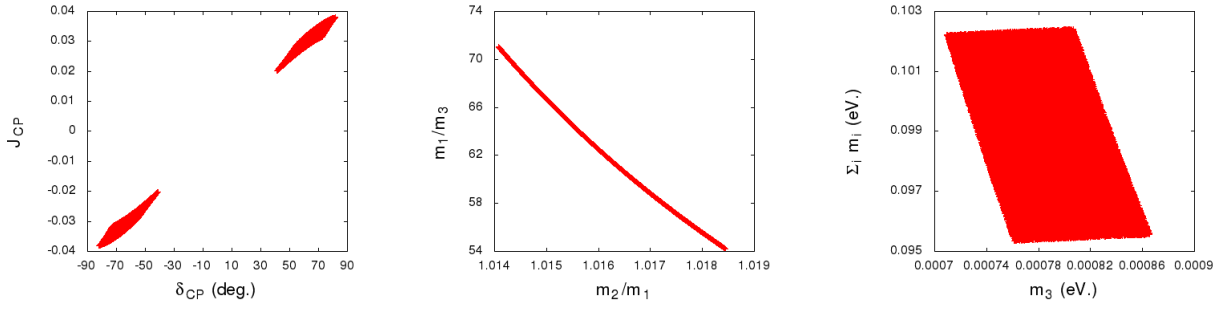


Figure 4: (colour online) The first one shows the variation of J_{CP} with δ_{CP} , the second one stands for the inverted hierarchy of neutrino masses and last one shows a correlation between $\Sigma_i m_i$ with m_3 and all the plots presented in this figure are same for both the cases.

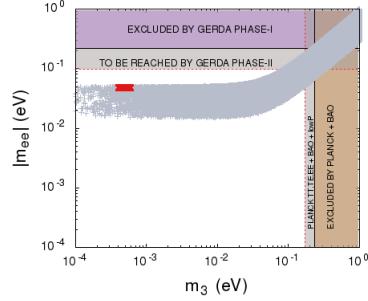


Figure 5: (colour online) Lightest eigenvalue (m_3) Vs $|m_{ee}|$ plot. The gray band shows the range of $|m_{ee}|$ allowed by the present oscillation data with all the CP phases within the range $0 - 2\pi$. The small red coloured band is allowed in our model.

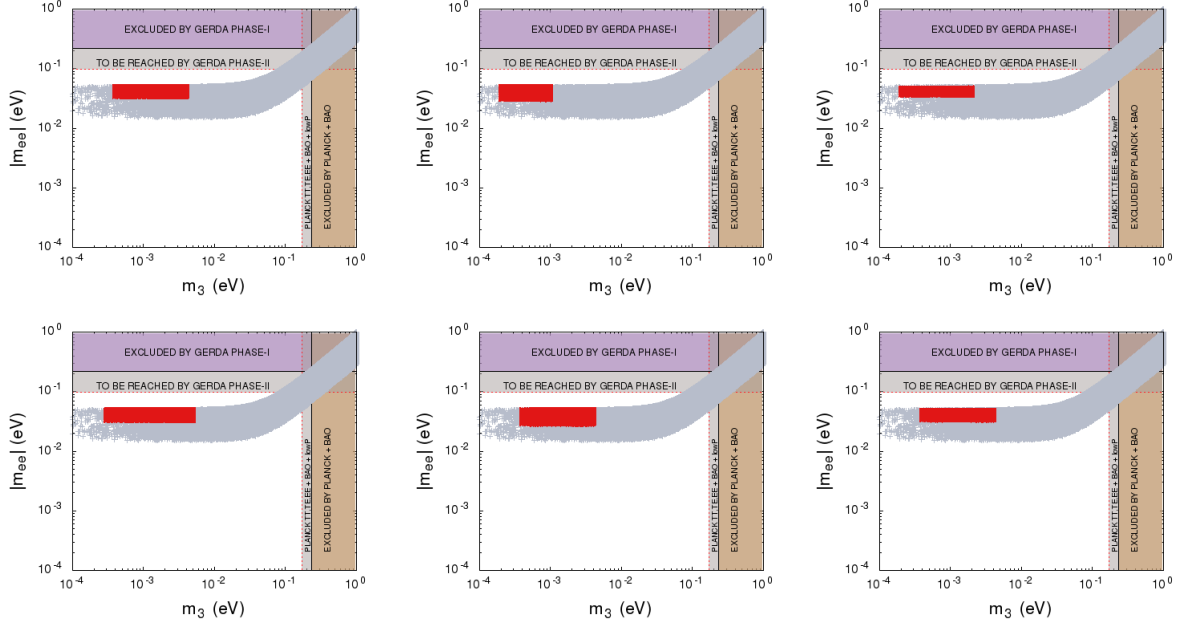


Figure 6: (colour online) Lightest eigenvalue (m_3) Vs $|m_{11}|$ plot: For all nondegenerate eigenvalues of M_{RS} . The first three figures of the first row are shown for the matrices $m_{\nu f12}^{i(=1,2,3)}$ and the figures in the second row are shown for the matrices $m_{\nu f13}^{i(=1,2,3)}$.

- [26] G. C. Branco, D. Emmanuel-Costa, M. N. Rebelo and P. Roy, Phys. Rev. D **77** (2008) 053011 [arXiv:0712.0774 [hep-ph]].
- [27] S. Choubey, W. Rodejohann and P. Roy, Nucl. Phys. B **808**, 272 (2009) [Erratum-ibid. **818**, 136 (2009)] [arXiv:0807.4289 [hep-ph]].
- [28] M. Chakraborty, H. Z. Devi and A. Ghosal, Phys. Lett. B **741**, 210 (2015) arXiv:1410.3276 [hep-ph].
- [29] B. Adhikary, A. Ghosal and P. Roy, JHEP **0910** (2009) 040 [arXiv:0908.2686 [hep-ph]].
- [30] B. Adhikary, A. Ghosal and P. Roy, JCAP **1101** (2011) 025 [arXiv:1009.2635 [hep-ph]].
- [31] B. Adhikary, A. Ghosal and P. Roy, Mod. Phys. Lett. A **26** (2011) 2427 [arXiv:1103.0665 [hep-ph]].
- [32] A. Ghosal and R. Samanta, JHEP **1505**, 077 (2015) [arXiv:1501.00916 [hep-ph]].
- [33] R. Samanta, M. Chakraborty and A. Ghosal, arXiv:1502.06508 [hep-ph].
- [34] P.F Harrison, D.H Perkins and D.G Scott, PLB **349**(1995) 137-144.
- [35] B. Adhikary, M. Chakraborty and A. Ghosal, JHEP **1310**, 043 (2013) [JHEP **1409**, 180 (2014)] [arXiv:1307.0988 [hep-ph]].
- [36] B. Adhikary, M. Chakraborty and A. Ghosal, arXiv:1407.6173 [hep-ph].
- [37] S. Pramanick and A. Raychaudhuri, Phys. Rev. D **88**, no. 9, 093009 (2013) [arXiv:1308.1445 [hep-ph]].
- [38] Y. Koide, hep-ph/0005137.
- [39] A. Damanik, M. Satriawan, P. Anggraita, A. Hermanto and Muslim, J. Theor. Comput. Stud. **8**, 0102 (2008) [arXiv:0710.1742 [hep-ph]].
- [40] Y. Koide, J. Phys. G **34**, 1653 (2007) [hep-ph/0605074].

- [41] V. D. Barger, S. Pakvasa, T. J. Weiler and K. Whisnant, Phys. Lett. B **437**, 107 (1998) [hep-ph/9806387].
- [42] J. K. Elwood, N. Irges and P. Ramond, Phys. Rev. Lett. **81**, 5064 (1998) [hep-ph/9807228].
- [43] A. Ghosal, Phys. Rev. D **62**, 092001 (2000) [hep-ph/0004171].
- [44] B. C. Allanach, Phys. Lett. B **450**, 182 (1999) [hep-ph/9806294].
- [45] A. Ghosal, Mod. Phys. Lett. A **19**, 2579 (2004). doi:10.1142/S0217732304014951
- [46] A. Ghosal, hep-ph/0304090.
- [47] J. Iizuka, Y. Kaneko, T. Kitabayashi, N. Koizumi and M. Yasue, Phys. Lett. B **732**, 191 (2014) [arXiv:1404.0735 [hep-ph]].
- [48] T. Kitabayashi and M. Yasue, Phys. Lett. B **726**, 356 (2013) [arXiv:1309.0285 [hep-ph]].
- [49] C. Duarah, A. Das and N. N. Singh, Phys. Lett. B **718**, 147 (2012) [arXiv:1207.5225 [hep-ph]].
- [50] S. Dev, R. R. Gautam and L. Singh, Phys. Rev. D **89**, no. 1, 013006 (2014) [arXiv:1309.4219 [hep-ph]].
- [51] E. Ma and R. Srivastava, Phys. Lett. B **741**, 217 (2015) [arXiv:1411.5042 [hep-ph]].
- [52] E. Ma, N. Pollard, R. Srivastava and M. Zakeri, arXiv:1507.03943 [hep-ph].
- [53] Y. Muramatsu, T. Nomura and Y. Shimizu, JHEP **1603**, 192 (2016) doi:10.1007/JHEP03(2016)192 [arXiv:1601.04788 [hep-ph]].
- [54] B.Z Hu et al. (Daya Bay Collaboration), Phys. Rev. Lett. **115**, 111802 (2015) and references therein.
- [55] J. Liao, D. Marfatia and K. Whisnant, Nucl. Phys. B **900**, 449 (2015) doi:10.1016/j.nuclphysb.2015.09.020 [arXiv:1508.07364 [hep-ph]].
- [56] Y. Shimizu and M. Tanimoto, JHEP **1512**, 132 (2015) doi:10.1007/JHEP12(2015)132 [arXiv:1507.06221 [hep-ph]].
- [57] B. Adhikary and A. Ghosal, Phys. Rev. D **78**, 073007 (2008) doi:10.1103/PhysRevD.78.073007 [arXiv:0803.3582 [hep-ph]].
- [58] S. F. Ge, H. J. He and F. R. Yin, JCAP **1005**, 017 (2010) doi:10.1088/1475-7516/2010/05/017 [arXiv:1001.0940 [hep-ph]].
- [59] B. Adhikary, B. Brahmachari, A. Ghosal, E. Ma and M. K. Parida, Phys. Lett. B **638**, 345 (2006) doi:10.1016/j.physletb.2006.05.051 [hep-ph/0603059].
- [60] G. Altarelli, F. Feruglio and I. Masina, Nucl. Phys. B **689**, 157 (2004) [hep-ph/0402155].
- [61] D. V. Forero, M. Tortola and J. W. F. Valle, Phys. Rev. D **90**, no. 9, 093006 (2014) [arXiv:1405.7540 [hep-ph]].
- [62] P. A. R. Ade *et al.* [Planck Collaboration], Astron. Astrophys. **571**, A16 (2014) [arXiv:1303.5076 [astro-ph.CO]].
- [63] R. Samanta, P. Roy and A. Ghosal, arXiv:1604.01206 [hep-ph].
- [64] K. Ieki, T2K-THESIS-040.
- [65] J. Lesgourgues and S. Pastor, New J. Phys. **16**, 065002 (2014) [arXiv:1404.1740 [hep-ph]].
- [66] Audren B, Lesgourgues J, Bird S, Haehnelt M G and Viel M 2013 J. Cosmol. Astropart. Phys. JCAP01(2013)026
- [67] R. Samanta, P. Roy and A. Ghosal, arXiv:1604.06731 [hep-ph].